Title

Max Varverakis

March 12, 2024

Contents

Chapter 3

The Braid Group

Definition 3.1. The *configuration space* of n ordered distinct points in the complex plane $\mathbb{C}$ is defined as $M_n = \{(z_1, \ldots, z_n) \in \mathbb{C}; z_i \neq z_j, \forall i \neq j\}$. Alternatively, consider $\mathcal{D}$ to be the collection of all hyperplanes $H_{i,j} = \{z_i = z_j\} \in \mathbb{C}^n$ for $1 \leq i < j \leq n$. Then we can define $M_n = \mathbb{C}^n \setminus \mathcal{D}$.

Note that $(z_1, z_2, z_3, \ldots, z_n)$ and $(z_2, z_1, z_3, \ldots, z_n)$ are different points in the configuration space M_n. Before studying the various interpretations of the braid group, we first define the braid group itself.

Definition 3.2. The *pure braid group* on n strands, denoted PB_n, is the fundamental group of M_n. One can write $PB_n = \pi_1(M_n)$.

3.1 Visualization of pure braids

We can think of a pure braid as a loop in M_n:

$$\begin{aligned} \beta : [0,1] &\to M_n \\ t &\mapsto \beta(t) = (\beta_1(t), \beta_2(t), \ldots, \beta_n(t)) \,, \end{aligned}$$

with some base point. Conventionally, we define the base point as the n-tuple of integers $(1, 2, 3, \ldots, n) \in \mathbb{C}^n$. Then a pure braid can be though of the motion of these points in the complex plane as t ranges from 0 to 1 in which $\beta_i(t)$ is defined and $\beta_i(t) \neq \beta_j(t)$ for every $t \in [0,1]$ and $i \neq j \in \{1, 2, \ldots, n\}$. Because each β_i is a loop, it must start and end at the point

i (e.g., $\beta_i(0) = \beta_i(1) = i$). Recall that the loops are actually equivalence classes of loops under homotopy. As a result, we can continuously deform the motion of the n points while maintaining the same pure braid (up to equivalence) so long as we preserve the pairwise distinction of the points for all time $t \in [0, 1]$.

A common visualization of pure braids is to plot the motion of the points in 3-dimensional space. For each $t \in [0, 1]$, we draw the points $(\beta_i(t), t)$ in $\mathbb{C} \times [0, 1]$ for every $i \in \{1, \ldots, n\}$. The space $\mathbb{C} \times [0, 1]$ can be thought of as a spacetime diagram, where the motion of the points is plotted in the complex plane at each time t, with the time being the vertical axis. The convention is to have $\mathbb{C} \times \{0\}$ placed above $\mathbb{C} \times \{1\}$, so that the motion of the points is plotted from top to bottom, as in Figure 3.1.

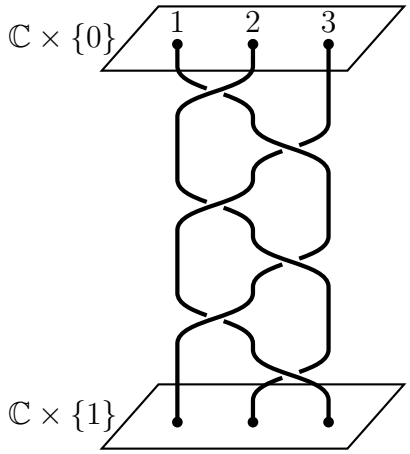

Figure 3.1: A pure braid on three strands is visualized as the trajectory of three particles as they move in $\mathbb{C}$, plotted over an arbitrary (normalized) time period. Each point ends at the same relative starting position in $\mathbb{C}$.

For every $i \in \{1, \ldots, n\}$, the motion of a single point starting at $(i, 0)$ and ending at $(i, 1)$ is known as the i-th *strand* of the pure braid. This can also be described by the i-th projection of the n-tuple $\beta(t)$. Thus, two braids are equivalent under homotopy if, for every moment of a continuous deformation of the n strands in $\mathbb{C} \times [0, 1]$, the (fixed) endpoints $((1, 0), (2, 0), \ldots, (n, 0))$ and $((1, 1), (2, 1), \ldots, (n, 1))$ are connected by strands that are pairwise disjoint where each strand intersects the plane $\mathbb{C} \times \{t\}$ exactly once for every $t \in [0, 1]$.

As pure braids are members of the pure braid group, multiplication is a well-defined operation. In the context of M_n, multiplication of pure braids involves the concatenation of loops. Visually, this is the process of stacking braids on top of each other, and then rescaling the time dimension so that t ranges from 0 to 1.

3.2 General braids

In the previous section, we defined pure braids in which the endpoints of each strand are identical at the beginning and end of the motion. This notion generalizes to define (non-pure) braids. First, we define a more general configuration space than M_n. The symmetric group S_n permutes the n distinct points in $\mathbb{C}$. Then the *configuration space of n unordered points in* $\mathbb{C}$ is the quotient space $N_n = M_n/S_n$.

Definition 3.3. The braid group on n strands is the fundamental group of N_n, denoted $B_n = \pi_1(N_n)$.

The visualization of a braid is the same as in the case of pure braids, only now the endpoints of each strand do not necessarily match the starting points, as illustrated Figure 3.2. For example, the i-th strand may start at the point $(i, 0)$ but end at the point $(j, 1)$ for $i, j \in \{1, \ldots, n\}$. The equivalence of strands is still defined as before under the homotopy of loops. Loop concatenation defines the multiplication of braids, as before.

Note that for $n \geq 1$ there is a natural inclusion $\iota : B_n \hookrightarrow B_{n+1}$ in which we add a new strand to any $\beta \in B_n$ that does not interact with the other strands.

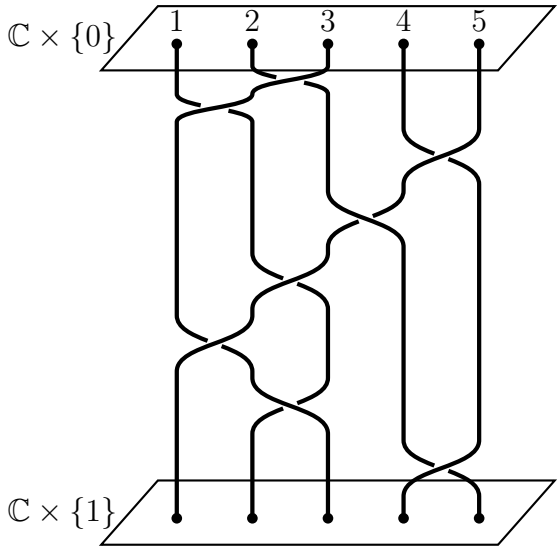

Figure 3.2: A general braid on five strands. The ending position of each particle is not necessarily in the same location of $\mathbb{C}$ as the starting position, which classifies this as a general braid.

3.3 Standard generators of the braid group

Originally proposed by Artin [1], each braid can be decomposed into a product of *standard generators* of the braid group. When visualizing braids in $\mathbb{R} \times [0, 1]$, a crossing of two strands is clearly indicated by one going over the other, as in Figure 3.3. Suppose each crossing occurs at a different time $t \in [0, 1]$. Then by rescaling the time component of an arbitrary braid, we can decompose it into a stack of simple braids with only one crossing between neighboring strands per braid. Each single crossing of strands can be obtained by performing a transposition between neighboring endpoints of the strands.

For instance, swapping the endpoints of the i-th and $(i+1)$-th strands can be written as applying σ_i to the identity braid (i.e., the braid that starts without any crossings of strands). It must be noted that there are two distinct ways to swap the endpoints of two strands. From a top-down perspective looking at the plane $\mathbb{C} \times \{t\}$ for some time t, σ_i swaps (i, t) and $(i+1, t)$ in a clockwise rotation. The reverse of this operation (i.e., twisting the endpoints around in the counterclockwise direction) is denoted σ_i^{-1}. Both of these operations are

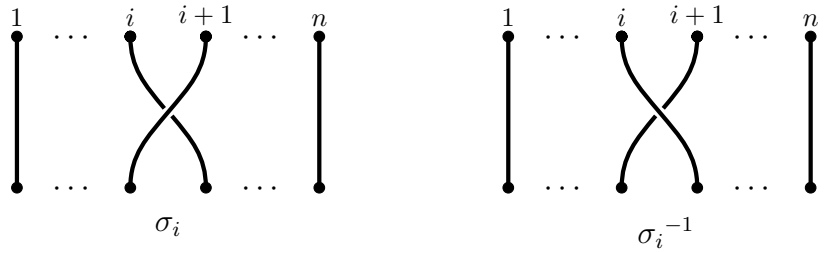

Figure 3.3: The action of σ_i on n strands. The i-th strand gets twisted behind the $(i+1)$-th strand when acted on by σ_i, and the opposite occurs for ${\sigma_i}^{-1}$. In that way, concatenating these two braids would result in no intertwining of strands, giving the identity braid.

illustrated in Figure 3.3. The standard generators of the braid group B_n are defined as the set $\{\sigma_1, \sigma_2, \ldots, \sigma_{n-1}\}$. An arbitrary braid can be constructed by concatenating (or stacking) the simple braids made from the standard generators before rescaling the time coordinate to $[0, 1]$.

3.4 Automorphisms of the free group

Consider the n-times punctured disk $\mathbb{D}_n$. The fundamental group of $\mathbb{D}_n$ involves loops that start and end at the same (fixed) base point in $\partial\mathbb{D}_n$. Up to homotopy, a clockwise-directional loop that encompasses the i-th hole in $\mathbb{D}_n$ corresponds to the i-th generator of the free group F_n of rank n, which is illustrated in Figure 3.4. In fact, $\pi_1(\mathbb{D}_n) = F_n$. This equality allows us to define a representation of the braid group on n strands as automorphisms of F_n.

Each braid $\beta \in B_n$ is realized as an automorphism of $\pi_1(\mathbb{D}_n) = F_n$ (up to isotopy) where each loop $\gamma \in \pi_1(\mathbb{D}_n)$ is sent to another loop $\beta(\gamma)$. In other words, we have a representation of the braid group defined by

$$\rho : B_n \to \mathrm{Aut}(F_n) \tag{3.1}$$

$$\beta \mapsto \rho_\beta. \tag{3.2}$$

The action of β on a loop γ is defined by the rearrangements of the n holes in $\mathbb{D}_n$, similar to the action of the standard generators of B_n on the base points in $\mathbb{C} \times \{1\}$. In terms of the standard generators of B_n, each σ_i corresponds to

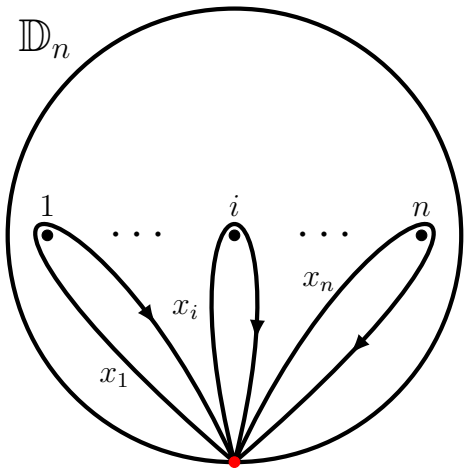

Figure 3.4: For each $i \in \{1, \ldots, n\}$, the clockwise-directional loop encircling the i-th hole in $\mathbb{D}_n$ corresponds to the i-th free generator of F_n (i.e., x_i). The red dot indicates the (arbitrary) base point for the loops in $\pi_1(\mathbb{D}_n)$.

switching the places of hole i and hole $i+1$ by means of a clockwise rotation, as seen in Figure 3.5. This is identical to viewing the action of σ_i on the base points (Section 3.3) from above, looking down on the $\mathbb{C} \times \{t\}$-plane. As before, the inverse action ${\sigma_i}^{-1}$ is a counterclockwise rotation of the two adjacent holes i and $i+1$ in $\mathbb{D}_n$. These actions respect the group operation of loop concatenation.

Note that there is not a widely accepted convention for the standard generators of the braid group. For example, many sources will define the direction of the standard generators to be counterclockwise, where the punctures on $\mathbb{D}_n$ are swapped in the opposite manner as in this thesis. Moreover, when considering the braid group as the intertwining of strands in $\mathbb{C} \times [0, 1]$, a generator σ_i may be defined as overlaying the i-th strand in front of the $(i+1)$-th strand rather than behind. This is a matter of convention, and the choice of the standard braid permutations is equivalent up to inverses.

The automorphism ρ_β is most simply defined in terms of the action of the standard generators of B_n on the generators $x_1, \ldots, x_n$ of F_n (visualized as

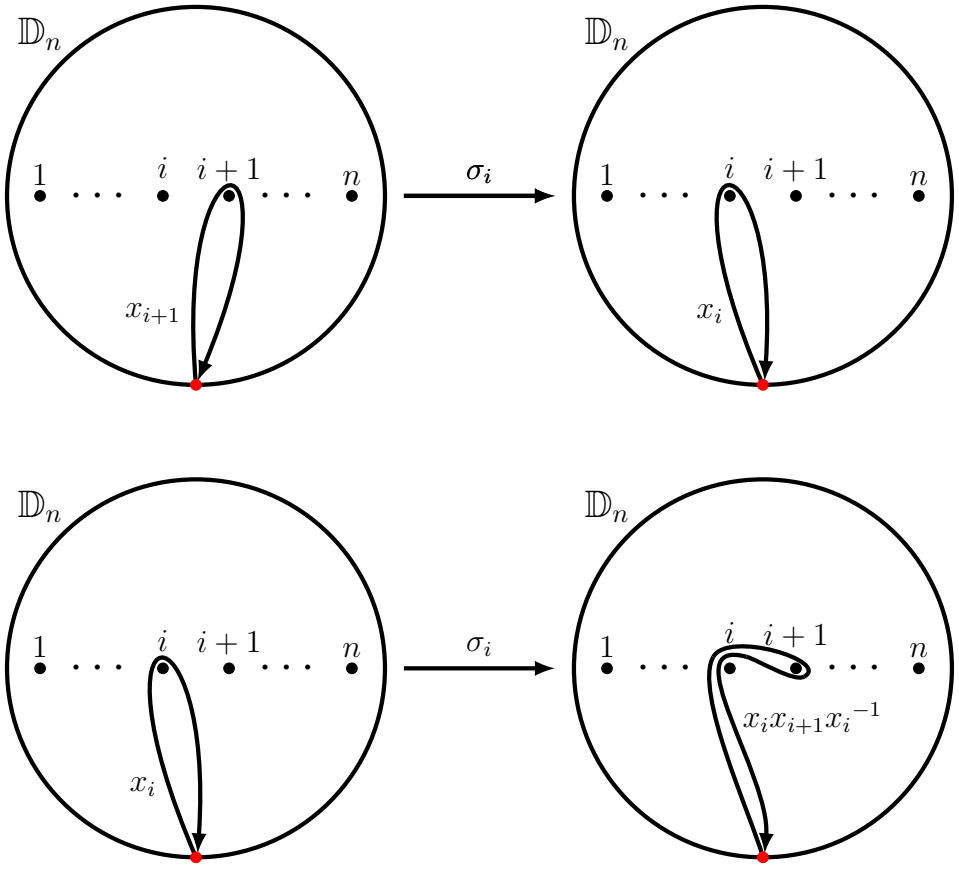

Figure 3.5: The action of σ_i on the generators x_i and x_{i+1} as described by Eqns. 3.3–3.5. The image of x_i under σ_i is verified visually in Figure 3.6

loops in $\mathbb{D}_n$). For each i, it follows that

$$\rho_{\sigma_i}(x_i) = x_i x_{i+1} x_i^{-1}, \tag{3.3}$$
$$\rho_{\sigma_i}(x_{i+1}) = x_i, \tag{3.4}$$
$$\rho_{\sigma_i}(x_j) = x_j, \text{ for } j \neq i, i-1. \tag{3.5}$$

Clearly, any two loops that are separated by at least one puncture will not interact while performing σ_i. The relations for adjacent loops can be verified graphically as illustrated in Figures 3.5 and 3.6.

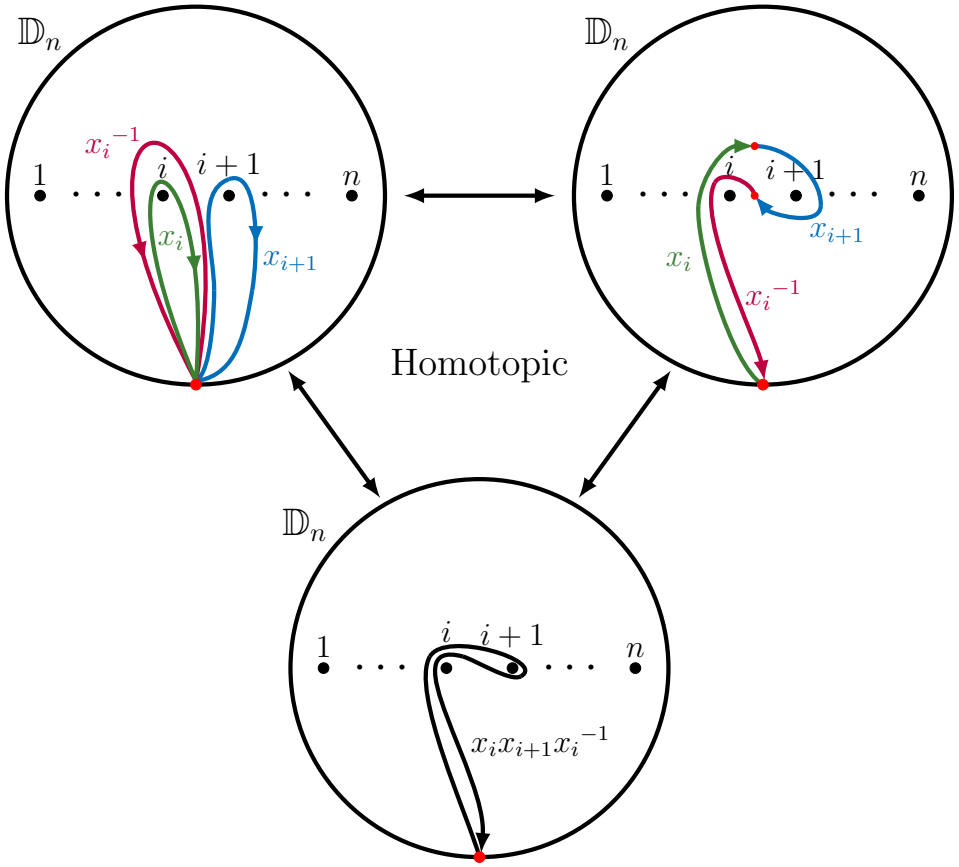

Figure 3.6: Up to homotopy, the product $x_i x_{i+1} x_i^{-1}$ is visualized as the concatenation of the loops $x_i, x_{i+1}, x_i^{-1} \in \pi_1(\mathbb{D}_n)$. In the top right diagram, small red dots are used indicate the (homotopically deformed) points of concatenation.

For any σ_i, $\rho_{\sigma_i{}^{-1}}$ is well-defined. It follows that for any braid $\beta \in B_n$, we can decompose ρ_β the composition of the automorphisms of the standard generators $\sigma_1, \ldots, \sigma_{n-1}$ and their inverses that make up β.

Notice that for any σ_i, $\rho_{\sigma_i}(x_1 \cdots x_n) = x_1 \cdots x_n$. This is because the loop $x_1 \cdots x_n$ in $\mathbb{D}_n$, encompassing all holes, is parallel to the boundary $\partial\mathbb{D}_n$. Thus, the action of σ_i on $x_1 \cdots x_n$ is trivial does not affect the structure of the loop up to isotopy. More generally, this implies that $\rho_\beta(x_1 \cdots x_n) = x_1 \cdots x_n$ for any $\beta \in B_n$. Paired with the observation that every generator is conjugate to another, Artin [1] showed that this is a necessary and sufficient condition for ρ_β to be an automorphism of F_n.

Theorem 3.1. *An automorphism $f \in Aut(F_n)$ is equal to ρ_β for some $\beta \in B_n$ if and only if*

1. *$f(x_i)$ is a conjugate of some x_j for every $i \in \{1, \ldots, n\}$, and*
2. *$f(x_1 \cdots x_n) = x_1 \cdots x_n$.*

In this interpretation of the braid group, we can express B_n in terms of the standard generators:

$$B_n = \left\langle \sigma_1, \ldots, \sigma_{n-1} \;\middle|\; \begin{array}{ll} \sigma_i\sigma_j = \sigma_j\sigma_i, & |i-j| > 1 \\ \sigma_i\sigma_{i+1}\sigma_i = \sigma_{i+1}\sigma_i\sigma_{i+1}, & |i-j| = 1 \end{array} \right\rangle. \tag{3.6}$$

The first condition that the standard generators commute if $|i - j| > 1$ is easily verified by thinking about the action of the generators on $\pi_1(\mathbb{D}_n)$ as in Figure 3.5 and as automorphisms in Eqn. 3.5. This follows from the fact that if punctures i and j are non-adjacent, then the actions of σ_i and σ_j are mutually exclusive and thus commutative. The second condition on the standard generators is most easily verified in Figure 3.7 by looking at the corresponding braids in $\mathbb{R} \times [0, 1]$ (here, the distinction between $\mathbb{R}$ and $\mathbb{C}$ is only a matter of choosing to show the starting and ending complex planes in traditional braid visualizations).

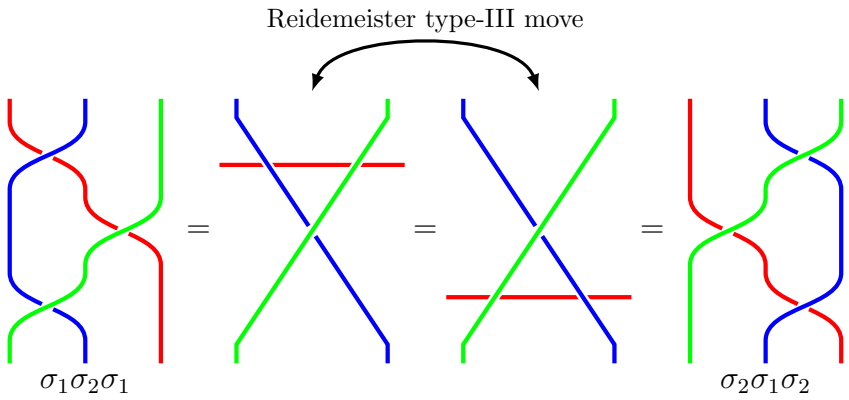

Figure 3.7: Graphical verification of Eqn. 3.6. All of the above braids are equivalent up to homotopy. The transformation between the middle two braid diagrams is known as a Reidmeister type-III move, in which the red strand (or string in the context of knot theory) is moved completely under the crossing of the blue and green strands. In these middle two diagrams, the red strand is slightly translucent to indicate that it is behind all other strands in the diagram.

3.5 One-dimensional representations of B_n

A straightforward nontrivial representation of the braid is defined on the standard generators of B_n and is given by [4]:

$$p_\theta : B_n \to \mathbb{C}_{|z|=1} \tag{3.7}$$

$$\sigma_i \mapsto e^{i\theta}, \tag{3.8}$$

for $\theta \in \mathbb{R}$. Clearly, p_θ is a homomorphism, and it is unitary because

$$p_\theta(\sigma_i)^\dagger = \left(e^{i\theta}\right)^\dagger = e^{-i\theta} = \left(e^{i\theta}\right)^{-1} = p_\theta(\sigma_i)^{-1}, \tag{3.9}$$

where † denotes the conjugate transpose of a matrix. Notice that with a choice of $\theta = 2\pi n$ for $n \in \mathbb{Z}$, we recover the trivial representation of B_n. Similarly, $p_{\pi n}$ is a restriction of the sign representation of S_n, where the sign of a permutation is defined as the parity of the number of transpositions in its decomposition into a product of transpositions.

3.6 The Burau Representation

In the previous section, we defined a representation of the braid group B_n as automorphisms of the free group F_n. This representation is clearly non-abelian. Likewise, the Artin generators of B_n are nonabelian. Suppose we wish to abelianize the braid group. The details of the abelianization of B_n would require a quotient by the commutator $[a, b] = aba^{-1}b^{-1}$.

Sparing the details, let $B_{n,ab} = B_n / [B_n, B_n]$ be the abelianization of B_n, where $[B_n, B_n] = \left\{ [\beta_1, \beta_2] \;\middle|\; \beta_1, \beta_2 \in B_n \right\}$ is the commutator subgroup of B_n. Then, under the representation ρ from Section 3.4, the abelianization of Eqns. 3.3–3.5 become

$$x_i \overset{\sigma_i}{\longmapsto} \cancel{x_i} + x_{i+1} - \cancel{x_i} = x_{i+1} = \rho_{{\sigma_i}^{-1}}(x_i), \tag{3.10}$$

$$x_{i+1} \overset{\sigma_i}{\longmapsto} x_i, \tag{3.11}$$

$$x_j \overset{\sigma_i}{\longmapsto} x_j, \text{ for } j \neq i, i-1, \tag{3.12}$$

for each i. Thus, the generator $\sigma_i = {\sigma_i}^{-1}$, and corresponds to a transposition permutation in the symmetric group S_n. It follows that $B_{n,ab} \simeq S_n$. In this current construction, the abelianization of the braid group results in a loss of complexity. This raises the question whether there exists such a reframing of the braid group that allows an abelian operation on the free generators while preserving the inequivalence of the Artin generators with their inverses.

First, we define a topological space that will aid in the desired construction.

Definition 3.4. Let X be a topological space. A *covering* of X is a space $\widetilde{X}$ together with a continuous map $p : \widetilde{X} \to X$ such that, for every $x \in X$, there exists a path-connected open neighborhood U containing x such that $p^{-1}(U)$ is a disjoint union of open sets in $\widetilde{X}$ where each component of $p^{-1}(U)$ is mapped homeomorphically onto U by p. Each component of $p^{-1}(U)$ is called a *sheet* of the covering, where the i-th sheet is denoted by $\widetilde{X}_i$, and total the number of sheets in $p^{-1}(U)$ is called the *degree* of the covering.

Example 3.1. One of the simplest examples of a covering space is the covering of the circle S^1 by the real line by the parameterization map $p : \mathbb{R} \to S^1$ defined by $p(t) = (\cos t, \sin t)$. Clearly, there are infinitely many sheets in this covering.

Example 3.2. A similar example is the covering of the circle S^1 through $p : [0, 1] \to S^1$ defined by $p(t) = e^{2\pi it}$. This defines a one-degree covering of S^1. If we instead let our domain be $[0, 2]$, then we have a two-degree covering of S^1.

With this topological tool, we construct a countably infinite-degree covering of the punctured disk $\mathbb{D}_n$, denoted $\widetilde{\mathbb{D}}_n$, which can be visualized as an infinite stack of copies of $\mathbb{D}_n$, with a slight modification to be explained shortly. Let $\widetilde{\mathbb{D}}_{n,i}$ denote the i-th sheet of $\widetilde{\mathbb{D}}_n$, and consider the base sheet our covering to be $\widetilde{\mathbb{D}}_{n,0}$.

We start this construction with a countably infinite stack of copies of $\mathbb{D}_n$. Then, for every $i \in \mathbb{Z}$, for each of the n punctures on $\widetilde{\mathbb{D}}_{n,i}$, apply a cut from the hole to some point on the boundary of $\widetilde{\mathbb{D}}_{n,i}$, as illustrated in Figure 3.8 for the case when $n = 3$. Each cut results in two edges, which will be referred to as the left edge and the right edge. Through a homeomorphic deformation, connect the left edge of $\widetilde{\mathbb{D}}_{n,i}$ to the corresponding right edge of $\widetilde{\mathbb{D}}_{n,i+1}$, and the right edge of $\widetilde{\mathbb{D}}_{n,i}$ to the left edge of $\widetilde{\mathbb{D}}_{n,i-1}$, for every cut on every sheet.

Now, viewing a single sheet, say $\widetilde{\mathbb{D}}_{n,0}$, from above, when a loop with base point $\tilde{\zeta}_0$ passes through a cut from the left, it traverses up to the next sheet, and ends at the base point $\tilde{\zeta}_1$. Similarly, a loop passing through a cut from the right ends at the base point $\tilde{\zeta}_{-1}$, on the sheet $\widetilde{\mathbb{D}}_{n,-1}$ below $\widetilde{\mathbb{D}}_{n,0}$. To keep track of the various loops, we use a free parameter t. For example, a loop γ that starts on $\widetilde{\mathbb{D}}_{n,j}$ would be written $t^j\gamma$, for $j \in \mathbb{Z}$. Notice that the substitution of a complex number for the free parameter t results in a possibly finite degree covering. As an example, if we set t to an n-th root of unity, then we obtain an n-th degree covering of $\mathbb{D}_n$. For the purposes of this construction, we will keep t as a free parameter for now. Figure 3.8 demonstrates how loops interact with the cuts on different sheets. The following example describes the action of the standard generators of B_3 on the covering space $\widetilde{\mathbb{D}}_3$.

Example 3.3. Consider the case when $n = 3$. Then we have the corresponding covering space $\widetilde{\mathbb{D}}_3$ of $\mathbb{D}_3$. See Figure 3.8 for the view of a single sheet with various loops interacting with the cuts on the sheet. The actions of the standard generators of B_3 in $\pi_1(\mathbb{D}_3)$ are known, and can be visually understood in Figure 3.5. In the context of the covering space $\widetilde{\mathbb{D}}_3$, the action of the generators σ_1 and σ_2 is observed by reducing the visualization to only the base points on each sheet and the loops themselves. This can be seen in

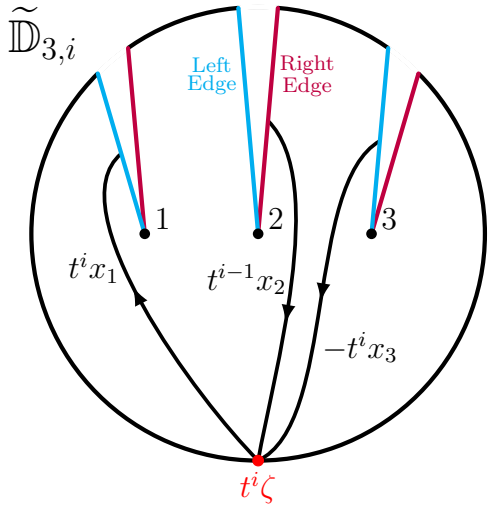

Figure 3.8: For the covering of $\mathbb{D}_3$, we observe the i-th sheet of $\widetilde{\mathbb{D}}_3$ with the cuts applied across each of the three punctures. The base point of the loop is indicated by the red dot, and labelled as $t^i\zeta$. The power of t indicates that we are on the i-th sheet of the covering. The portions of three different loops are drawn to illustrate the behavior of loops as they pass through various edges on $\widetilde{\mathbb{D}}_{3,i}$. The loop that would traditionally be x_1 is labeled by $t^i x_1$ to indicate that it's starting on the i-th sheet. When it passes through the left edge corresponding to this puncture labeled with a 1, it traverses up to the sheet $\widetilde{\mathbb{D}}_{3,i+1}$ and ends at base point $t^{i+1}\zeta$. Similarly, the loop that starts on $\widetilde{\mathbb{D}}_{3,i-1}$ and passes through the left edge of puncture 2 ends up coming out of the right edge of puncture 2 on $\widetilde{\mathbb{D}}_{3,i}$ and ends at the base point $t^i\zeta$. This loop is labeled by the starting sheet, so it is $t^{i-1}x_2$. Finally, the loop that starts on $\widetilde{\mathbb{D}}_{3,i+1}$ and passes through the right edge of puncture 3 ends up coming out of the left edge of puncture 3 on $\widetilde{\mathbb{D}}_{3,i}$. This loop is labeled by $-t^i x_3$ since it is the inverse of $t^i x_3$, with the negative sign indicating that the loop direction is reversed.

Figure 3.9 for the case of σ_1.

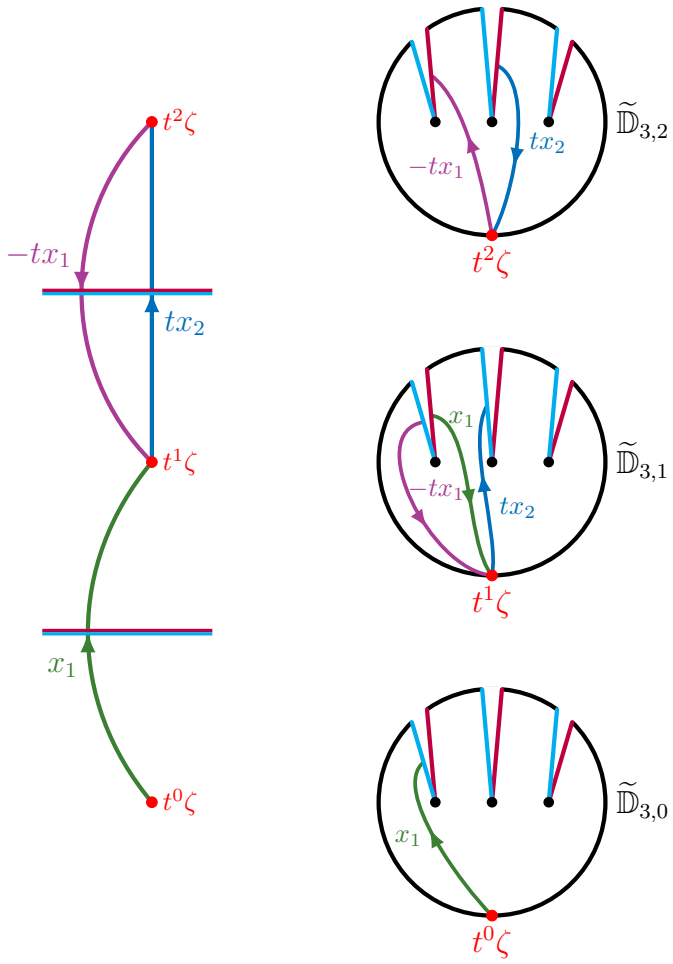

Figure 3.9: The loop $\rho_{\sigma_1}(x_1) = {x_1}^{-1}x_2x_1$ cast onto the covering space $\widetilde{\mathbb{D}}_3$. On the right, the loops are depicted on the corresponding sheets of the covering, and on the left is a simplified version. The order of loops is $x_1, tx_2, -tx_1$. The horizontal lines on the left indicate the edges taking each loop up/down a sheet.

Now, we can express loop concatenation as an abelian operation, where

Eqns. 3.3–3.5 become

$$x_1 \overset{\sigma_1}{\longmapsto} x_1 + tx_2 - tx_1 = (1-t)x_1 + tx_2, \tag{3.13}$$

$$x_2 \overset{\sigma_1}{\longmapsto} x_1, \tag{3.14}$$

$$x_3 \overset{\sigma_1}{\longmapsto} x_3. \tag{3.15}$$

Consider the vector $\begin{bmatrix} x_1 \\ x_2 \\ x_3 \end{bmatrix}$. Then the action of σ_1 on the loops x_1, x_2, x_3 is realized by the matrix $\begin{bmatrix} 1-t & t & 0 \\ 1 & 0 & 0 \\ 0 & 0 & 1 \end{bmatrix}$ since

$$\begin{bmatrix} 1-t & t & 0 \\ 1 & 0 & 0 \\ 0 & 0 & 1 \end{bmatrix} \begin{bmatrix} x_1 \\ x_2 \\ x_3 \end{bmatrix} = \begin{bmatrix} (1-t)x_1 + tx_2 \\ x_1 \\ x_3 \end{bmatrix}. \tag{3.16}$$

The action of σ_2 is obtained similarly, where

$$\sigma_2 \mapsto \begin{bmatrix} 1 & 0 & 0 \\ 0 & 1-t & t \\ 0 & 1 & 0 \end{bmatrix}. \tag{3.17}$$

Notice that these matrices have entries in the ring of Laurent polynomials, $\Lambda = \mathbb{Z}[t, t^{-1}]$.

Clearly, the result from Example 3.3 generalizes to the case of braids on n strands. Fix $n > 1$. Let I_k denote the $k \times k$ dimensional identity matrix, and let

$$U = \begin{bmatrix} 1-t & t \\ 1 & 0 \end{bmatrix}. \tag{3.18}$$

For $i \in \{1, \ldots, n-1\}$, the action of σ_i on $\pi_1\left(\widetilde{\mathbb{D}}_n\right)$ is realized as an $n \times n$ matrix with entries in $\Lambda = \mathbb{Z}[t, t^{-1}]$.

The Burau representation of B_n is then defined by:

$$\psi_n : B_n \to \mathrm{GL}_n(\Lambda) \tag{3.19}$$

$$\sigma_i \mapsto \begin{bmatrix} I_{i-1} & 0 & 0 \\ 0 & U & 0 \\ 0 & 0 & I_{n-i-1} \end{bmatrix}. \tag{3.20}$$

The Burau representation need only be defined on the standard generators, since any braid $\beta \in B_n$ decomposes into a product of $\sigma_1, \ldots, \sigma_{n-1}$ and their inverses. Notice that if we set $t \to 1$, we recover the defining representation of S_n, as expected when we use a degree 1 covering space of $\mathbb{D}_n$ and force the action of the generators to be abelian. Furthermore, by direct computation, it follows that

$$\psi_n(\sigma_i)\psi_n(\sigma_j) = \psi_n(\sigma_j)\psi_n(\sigma_i) \text{ for } |i-j| > 1, \tag{3.21}$$

$$\psi_n(\sigma_i)\psi_n(\sigma_{i+1})\psi_n(\sigma_i) = \psi_n(\sigma_{i+1})\psi_n(\sigma_i)\psi_n(\sigma_{i+1}) \text{ for } |i-j| = 1. \tag{3.22}$$

Moreover, the Burau representation is compatible with the natural inclusion map $\iota : B_n \hookrightarrow B_{n+1}$ for $n \geq 1$ and $\beta \in B_n$:

$$\psi_{n+1}(\iota(\beta)) = \begin{bmatrix} \psi_n(\beta) & 0 \\ 0 & 1 \end{bmatrix}. \tag{3.23}$$

3.7 The Reduced Burau Representation

Recall that in Section 3.4, every braid in B_n is described by an automorphism of the free group F_n. Equivalently, we thought of each generator σ_i as a clockwise rearrangement of adjacent punctures of $\mathbb{D}_n$ and recorded the resulting transformation of the n free generators of $F_n = \pi_1(\mathbb{D}_n)$, which were the loops around the punctures. It is intuitive to understand why the loop $\ell = x_1 \cdots x_n$ is invariant under any braid-realized automorphism, as the loop encompasses all n punctures in $\mathbb{D}_n$. This was discussed in Section 3.4, and was formalized in Theorem 3.1 as a necessary and sufficient condition for the realization of braids as automorphisms on the free group.

The invariant loop ℓ gives insight into the Burau representation. As was done with the generators $x_1, \ldots, x_n$ when constructing the Burau representation from $\pi_1(\mathbb{D}_n)$, the loop ℓ is written as an element of the free Λ-module of rank n, denoted Λ^n, when cast onto the covering space $\widetilde{\mathbb{D}}_n$:

$$x_1 \cdots x_n \in F_n \mapsto x_1 + tx_2 + t^2x_3 + \cdots + t^{n-1}x_n = \sum_{i=1}^{n} t^{i-1}x_i \in \Lambda^n. \tag{3.24}$$

The right-hand side of Eqn. 3.24 manifests as a vector $\vec{\nu} = [1, t, t^2, \ldots, t^{n-1}]^\top$, where the vector components correspond to the coefficients of the free generators $x_1, \ldots, x_n$. Note that this vector comes from the coordinate representation of Λ^n rather than directly from a vector space since Λ is not a field,

but this serves as useful way to describe the elements of Λ^n. The coordinate description of Λ^n is useful in constructing a non-trivial invariant vector space with respect to the Burau representation.

In particular, notice that for any $\sigma_i \in B_n$, the matrix representation $\psi_n(\sigma_i)$ leaves $\vec{\nu}$ invariant. This can be verified directly by computing the matrix multiplication:

$$\begin{aligned}
\psi_n(\sigma_i)\vec{\nu} &= \begin{bmatrix} I_{i-1} & 0 & 0 \\ 0 & U & 0 \\ 0 & 0 & I_{n-i-1} \end{bmatrix} \begin{bmatrix} 1 \\ \vdots \\ t^{i-1} \\ t^i \\ \vdots \\ t^{n-1} \end{bmatrix} \\
&= \begin{bmatrix} I_{i-1} & 0 & 0 & 0 \\ 0 & 1-t & t & 0 \\ 0 & 1 & 0 & 0 \\ 0 & 0 & 0 & I_{n-i-1} \end{bmatrix} \begin{bmatrix} 1 \\ \vdots \\ t^{i-1} \\ t^i \\ \vdots \\ t^{n-1} \end{bmatrix} \\
&= \begin{bmatrix} 1 \\ \vdots \\ t^{i-1} - t^i + t^i \\ t^i \\ \vdots \\ t^{n-1} \end{bmatrix} = \begin{bmatrix} 1 \\ \vdots \\ t^{i-1} \\ t^i \\ \vdots \\ t^{n-1} \end{bmatrix} = \vec{\nu},
\end{aligned}$$

for $i = 1, 2, \ldots, n-1$. Since $\vec{\nu}$ is invariant under the generators of B_n, it is also invariant under any arbitrary braid in B_n. Therefore, we have a non-trivial ψ_n-invariant subspace defined by span $\{\vec{\nu}\}$, which implies that ψ_n is reducible (provided $n > 1$).

The goal of the following procedure is to obtain an irreducible representation of B_n from the Burau representation. First, given the invariance of $\vec{\nu}$ under ψ_n, we find a basis for a ψ_n-invariant vector space by looking for eigenvalues of $\psi_n(\sigma_i)$ for $i = 1, 2, \ldots, n-1$ [3]. Let $\vec{v}_i$ be defined as the vector with i-th component $-t$, $(i+1)$-th component equal to 1, and all other components

equal to zero, for $i = 1, 2, \ldots, n-1$. Again, by direct computation, we can verify that $\vec{v}_i$ is an eigenvector of $\psi_n(\sigma_i)$ with eigenvalue $-t$:

$$\psi_n(\sigma_i)\vec{v}_i = \begin{bmatrix} I_{i-1} & 0 & 0 & 0 \\ 0 & 1-t & t & 0 \\ 0 & 1 & 0 & 0 \\ 0 & 0 & 0 & I_{n-i-1} \end{bmatrix} \begin{bmatrix} 0 \\ \vdots \\ 0 \\ -t \\ 1 \\ 0 \\ \vdots \\ 0 \end{bmatrix} = \begin{bmatrix} 0 \\ \vdots \\ 0 \\ t^2 \\ -t \\ 0 \\ \vdots \\ 0 \end{bmatrix} = -t\vec{v}_i.$$

Proposition 3.2. *Define $\vec{v}_i$ as above. Then span $\{\vec{v}_i\}$ = span $\{\vec{v}_1, \vec{v}_2, \ldots, \vec{v}_{n-1}\}$ form a non-trivial $(n-1)$-dimensional ψ_n-invariant vector space.*

Proof. The vectors $\vec{v}_i$ are eigenvectors of $\psi_n(\sigma_i)$ with eigenvalue $-t$ for each $i = 1, 2, \ldots, n-1$. These eigenvectors are clearly linearly independent, and so span $\{\vec{v}_1, \vec{v}_2, \ldots, \vec{v}_{n-1}\}$ is a non-trivial $(n-1)$-dimensional vector space. Clearly $\psi_n(\sigma_i)\vec{v}_j = \vec{v}_j$ for $|i-j| > 1$, which is easily verified due to the block diagonal structure of ψ_n. Leveraging this block structure of $\psi_n(\sigma_i)$ also allows the following calculations

$$\begin{bmatrix} 1 & 0 & 0 \\ 0 & 1-t & t \\ 0 & 1 & 0 \end{bmatrix} \begin{bmatrix} -t \\ 1 \\ 0 \end{bmatrix} = \begin{bmatrix} -t \\ 1-t \\ 1 \end{bmatrix} = \begin{bmatrix} -t \\ 1 \\ 0 \end{bmatrix} + \begin{bmatrix} 0 \\ -t \\ 1 \end{bmatrix},$$
$$\begin{bmatrix} 1-t & t & 0 \\ 1 & 0 & 0 \\ 0 & 0 & 1 \end{bmatrix} \begin{bmatrix} 0 \\ -t \\ 1 \end{bmatrix} = \begin{bmatrix} -t^2 \\ 0 \\ 1 \end{bmatrix} = t \begin{bmatrix} -t \\ 1 \\ 0 \end{bmatrix} + \begin{bmatrix} 0 \\ -t \\ 1 \end{bmatrix},$$

which implies that

$$\psi_n(\sigma_i)\vec{v}_{i-1} = \vec{v}_{i-1} + \vec{v}_i,$$
$$\psi_n(\sigma_i)\vec{v}_{i+1} = -t\vec{v}_i + \vec{v}_{i+1}.$$

Therefore, $\{\vec{v}_1, \ldots, \vec{v}_{n-1}\}$ are $\psi_n(\sigma_i)$ invariant for all $i = 1, 2, \ldots, n-1$. Hence, span $\{\vec{v}_1, \ldots, \vec{v}_{n-1}\}$ is an $(n-1)$-dimensional ψ_n-invariant vector space. □

We can now define the reduced Burau representation in terms of the (unreduced) Burau representation:

$$\psi_n^{\mathbf{r}} : B_n \to \mathrm{GL}_{n-1}(\Lambda) \tag{3.25}$$

$$\sigma_i \mapsto \psi_n(\sigma_i)\big|_{\mathrm{span}\{\vec{v}_i\}}. \tag{3.26}$$

In practice, we find the actual matrices for $\psi_n^{\mathbf{r}}(\sigma_i)$ by means of a slightly different approach.

Go though derivation of V_i's or just state it?

not actually sure if these matrices come exactly from the same construction as above...

Let $V \in \mathrm{GL}_3(\Lambda)$ be defined by

$$V = \begin{bmatrix} 1 & t & 0 \\ 0 & -t & 0 \\ 0 & 1 & 1 \end{bmatrix}. \tag{3.27}$$

Then the reduced Burau representation matrices are given by

$$\psi_n^{\mathbf{r}}(\sigma_1) = \begin{bmatrix} -t & 0 & 0 \\ 1 & 1 & 0 \\ 0 & 0 & I_{n-3} \end{bmatrix}, \tag{3.28}$$

$$\psi_n^{\mathbf{r}}(\sigma_{n-1}) = \begin{bmatrix} I_{n-3} & 0 & 0 \\ 0 & 1 & t \\ 0 & 0 & -t \end{bmatrix}, \tag{3.29}$$

$$\psi_n^{\mathbf{r}}(\sigma_i) = \begin{bmatrix} I_{n-2} & 0 & 0 \\ 0 & V & 0 \\ 0 & 0 & I_{n-i-2} \end{bmatrix}, \tag{3.30}$$

for $i = 2, 3, \ldots, n-2$.

Prove invertible?

3.8 Unitary Representation Matrices

As explained in [3], we can use U from the construction of the (unreduced) Burau representation to show that there are no choices of the parameter

t such that the representation matrices are unitary. However, we can use the Burau representation matrices to construct a unitary representation of B_n [11].

First, let $t = s^2$ for some $s \in \mathbb{C}^*$. In other words, we are restricting t to be a square of a nonzero complex number. Define $n \times n$ matrix

$$P_{n-1} = \text{diag}(1, s, s^2, \ldots, s^{n-1}), \tag{3.31}$$

where diag denotes the diagonal matrix with the given diagonal entries. Furthermore, define $\psi_n^{\mathbf{s}}(\beta) = P_{n-1}\psi_n(\beta)(P_{n-1})^{-1}$ for $\beta \in B_n$. Note that

$$(P_{n-1})^{-1} = \text{diag}(1, s^{-1}, s^{-2}, \ldots, s^{-(n-1)}).$$

Due to the block structure of ψ_n as before,

$$\begin{aligned}\begin{bmatrix} s^i & 0 \\ 0 & s^{i+1} \end{bmatrix} U \begin{bmatrix} s^{-i} & 0 \\ 0 & s^{-i-1} \end{bmatrix} &= \begin{bmatrix} s^i & 0 \\ 0 & s^{i+1} \end{bmatrix} \begin{bmatrix} 1-s^2 & s^2 \\ 1 & 0 \end{bmatrix} \begin{bmatrix} s^{-i} & 0 \\ 0 & s^{-i-1} \end{bmatrix} \\ &= \begin{bmatrix} 1-s^2 & s \\ s & 0 \end{bmatrix}\end{aligned}$$

$$\psi_n^{\mathbf{s}}(\sigma_i) = P_{n-1}\psi_n(\sigma_i)(P_{n-1})^{-1}$$

for $\sigma_i \in B_n$, $i = 1, \ldots, n-1$.

SQUIER claims that this construction of $\psi_n^{\mathbf{s}}(\sigma_i)$ is unitary for all i.

3.9 Exercise from DELANEY

Here, Delaney has defined $\psi_{\mathbf{s}}(\beta) = P_{n-1}\psi_n^{\mathbf{r}}(\beta)(P_{n-1})^{-1}$

Suppose that for specific choices of $s \in \mathbb{C}^*$, we can decompose $J_{n-1}(s) = X^\dagger X$ for some $(n-1) \times (n-1)$ matrix X. Then

$$(J_{n-1}(s))^\dagger = \left(X^\dagger X\right)^\dagger = X^\dagger \left(X^\dagger\right)^\dagger = X^\dagger X = J_{n-1}(s),$$

which implies that $J_{n-1}(s)$ is Hermitian. In general, $J_{n-1}(s)$ is Hermitian if $s + s^{-1} \in \mathbb{R}$. In other words, either $s \in \mathbb{R}^*$, or if $s \in \mathbb{C}^*$, then

$$\begin{aligned} s + s^{-1} = \overline{s} + \overline{s^{-1}} &\iff s + \frac{\overline{s}}{|s|^2} = \overline{s} + \frac{s}{|s|^2} \\ &\iff s - \overline{s} = \frac{s - \overline{s}}{|s|^2} \\ &\iff |s| = 1, \end{aligned}$$

where $s\overline{s} = |s|^2$.

Thus, $s \in \mathbb{R} \cup \mathbb{C}_{|z|=1}$, which gives a more specific description of the diagonals of $J_{n-1}(s)$:

$$s + s^{-1} = s + \overline{s} = 2\mathrm{Re}(s), \tag{3.32}$$

where $\mathrm{Re}(z)$ denotes the real part of $z \in \mathbb{C}$. However, if J_{n-1} is to be decomposed into $X^\dagger X$, then we can further restrict the allowable values of s. Let $x_{i,j}$ denote the (i,j)-th entry of X. Then it must be that

$$2\mathrm{Re}(s) = \sum_{i=1}^{n-1} \overline{x}_{i,j} x_{i,j} = \sum_{i=1}^{n-1} |x_{i,j}|^2 \geq 0,$$

for all $j = 1, 2, \ldots, n-1$. Therefore, $\mathrm{Re}(s) > 0$. Furthermore, we place a restriction on X by observing that

$$\left(X^\dagger X\right)_{i,j} = \sum_{k=1}^{n-1} \overline{x}_{k,i} x_{k,j} = -\delta_{i,j\pm 1},$$

where δ_{ij} is the Kronecker delta.

For such a choice of s (hence X and t) and any braid $\beta \in B_n$, the corresponding matrix $X\psi_{\mathbf{s}}(\beta)X^{-1}$ is unitary.

Chapter 4

Anyons

The first few sections come from [8].

4.1 Two Non-Interacting Anyons

The interaction term in the Lagrangian for two anyons due to the braiding of the anyons is given by

$$\mathcal{L}_{\text{int}} = \hbar\alpha\dot{\phi}, \tag{4.1}$$

where a dot indicates a total time derivative $\frac{d}{dt}$ and $\phi = \arctan\left(\frac{y_2-y_1}{x_2-x_1}\right)$ is the relative angle between the two anyons with positions $\vec{r}_1 = (x_1, y_1)$ and $\vec{r}_2 = (x_2, y_2)$. As in the previous section, $\alpha \in [0, 1]$ is the *winding angle* or braiding statistic of the anyons. The parameter α can also be thought of as an angle modulo π. Though the relative angle ϕ is ambiguous for identical particles, the derivative $\frac{d\phi}{dt} = \dot{\phi}$ is well-defined.

Notice that if we take $\alpha \to 0$, the interaction term vanishes as expected for bosons. Similarly, for $\alpha > 0$, ϕ becomes singular if $\vec{r}_1 = \vec{r}_2$, which motivates the Pauli exclusion principle for fermions. In fact, this means that for any $\alpha > 0$, the corresponding anyons exhibit some form of the Pauli exclusion principle.

The classical kinetic energy of this system is

$$T = \frac{1}{2}m\left(\dot{\vec{r}}_1^{\,2} + \dot{\vec{r}}_2^{\,2}\right), \tag{4.2}$$

as expected. Then the Lagrangian for this system is

$$\mathcal{L}\left(\dot{\vec{r}}_1, \dot{\vec{r}}_2, \dot{\phi}\right) = T + \mathcal{L}_{\text{int}} = \frac{1}{2}m\left(\dot{\vec{r}}_1{}^2 + \dot{\vec{r}}_2{}^2\right) + \hbar\alpha\dot{\phi}, \tag{4.3}$$

which can also be viewed as the Lagrangian for 2 interacting bosons/fermions.

We can redefine the Lagrangian in terms of the relative and center-of-mass coordinates

$$\vec{R} = \frac{\vec{r}_1 + \vec{r}_2}{2}, \tag{4.4}$$

$$\vec{r} = \vec{r}_1 - \vec{r}_2, \tag{4.5}$$

where $\vec{r}$ is the relative position vector and $\vec{R}$ is the center-of-mass position vector of the two anyons. Note that we are assuming that the mass of the two particles are equal ($m_1 = m_2$). Classically, the momentum of a particle is given by the product of its mass and velocity. Then the corresponding center-of-mass and relative momenta:

$$\vec{P} = 2m\dot{\vec{R}} = 2m\frac{\vec{r}_1 + \vec{r}_2}{2} = m\dot{\vec{r}}_1 + m\dot{\vec{r}}_2 = \vec{p}_1 + \vec{p}_2, \tag{4.6}$$

$$\vec{p} = \mu\dot{\vec{r}} = \frac{m}{2}\left(\dot{\vec{r}}_1 - \dot{\vec{r}}_2\right) = \frac{\vec{p}_1 - \vec{p}_2}{2}, \tag{4.7}$$

where m is the mass of each anyon and μ is the reduced mass of the system.

With this in mind, we derive the following identity:

$$\dot{\vec{R}} + \frac{1}{4}\dot{\vec{r}} = \frac{\left(\dot{\vec{r}}_1 + \dot{\vec{r}}_2\right)^2}{4} + \frac{\left(\dot{\vec{r}}_1 - \dot{\vec{r}}_2\right)^2}{4} = \frac{\dot{\vec{r}}_1{}^2 + \dot{\vec{r}}_2{}^2}{2}. \tag{4.8}$$

Thus, the Lagrangian decomposes into relative and center-of-mass components upon making the substitution from the above identity:

$$\mathcal{L} = \underbrace{m\dot{\vec{R}}^2}_{\mathcal{L}_R} + \underbrace{\frac{m\dot{\vec{r}}^2}{4} + \hbar\alpha\dot{\phi}}_{\mathcal{L}_r}, \tag{4.9}$$

where the squared velocities indicate magnitude squared. Observe that the center-of-mass component of the Lagrangian, $\mathcal{L}_R$, is independent of the braiding parameter α. We can further simplify the relative component of the Lagrangian, $\mathcal{L}_r$, by noting that we can briefly write the coordinate $\vec{r}$ in polar form by representing it as a complex number $\vec{r} = re^{i\phi}$. It follows that

$$\left|\dot{\vec{r}}(r,\phi)\right|^2 = \left|\frac{d}{dt}\vec{r}(r,\phi)\right|^2 = \left|\left(\dot{r} + ir\dot{\phi}\right)e^{i\phi}\right|^2 = \dot{r}^2 + r^2\dot{\phi}^2. \tag{4.10}$$

Hence, we rewrite the relative component of the Lagrangian as

$$\mathcal{L}_r = \frac{m\left(\dot{r}^2 + r^2\dot{\phi}^2\right)}{4} + \hbar\alpha\dot{\phi}. \tag{4.11}$$

Recall that the classical relative angular momentum can be described by:

$$p_\phi = \frac{d\mathcal{L}}{d\dot{\phi}} = \frac{mr^2}{2}\dot{\phi} + \hbar\alpha. \tag{4.12}$$

Now, the Hamiltonian for this system can be constructed:

$$\begin{aligned}\mathcal{H} &= P\dot{R} + p_r\dot{r} + p_\phi\dot{\phi} - \mathcal{L} \\ &= \frac{P^2}{4m} + \frac{p_r^2}{m} + \frac{mr^2}{4}{p_\phi}^2 \\ &= \frac{P^2}{4m} + \frac{p_r^2}{m} + \frac{\left(p_\phi - \hbar\alpha\right)^2}{mr^2}.\end{aligned} \tag{4.13}$$

Once again, the center-of-mass component of the Hamiltonian is independent of α, and so we can focus on the relative component of the Hamiltonian, which is

$$\mathcal{H}_r = \frac{p_r^2}{m} + \frac{\left(p_\phi - \hbar\alpha\right)^2}{mr^2}. \tag{4.14}$$

For the purposes of this work, we need not carry out to find the energy eigenstates corresponding to the quantum operator of this relative Hamiltonian. More about this is found in [8].

4.2 Anyons in Harmonic Potential

The Hamiltonian for this system requires modification from previous sections when the anyons are placed in a harmonic potential. The potential energy of a 2-anyon system is given by

$$V(\vec{r}_1, \vec{r}_2) = \frac{1}{2} m\omega^2 \left(\vec{r}_1^{\,2} + \vec{r}_2^{\,2}\right) = m\omega^2 \left(\vec{R}^2 + \frac{1}{4}\vec{r}^{\,2}\right), \tag{4.15}$$

where ω is the angular frequency of the harmonic potential. We can make the same substitution as in the previous section to write the potential in terms of the relative and center-of-mass coordinates. As is the recurring theme, the center-of-mass component of the potential has no dependence on the braiding parameter α, and corresponds to a 2-dimensional quantum harmonic oscillator problem for a particle of mass $2m$.

Note that we can generalize Eqn. 4.11 (now omitting the subscript r) to an N-anyon system in a harmonic potential by writing

$$\mathcal{L} = \sum_{i=1}^{N} \frac{m}{2} \dot{\vec{r}}_i^{\,2} + \hbar\alpha \sum_{i \neq j} \dot{\phi}_{ij} - \frac{m\omega^2}{2} \sum_{i=1}^{N} \vec{r}_i^{\,2}, \tag{4.16}$$

where $\phi_{ij} = \arctan\left(\frac{y_i - y_j}{x_i - x_j}\right)$ is the relative angle between anyons i and j.

From [2], after rescaling our distance in units of $\sqrt{\frac{\hbar}{m\omega}}$, we can rewrite the Lagrangian as

$$\mathcal{L} = \frac{1}{2} \sum_{i=1}^{N} \left[\dot{\vec{r}}^{\,2} - \vec{r}_i^{\,2}\right] + \alpha \sum_{i<j}^{N} \frac{\vec{r}_{ij} \times \dot{\vec{r}}_{ij}}{r_{ij}^2}, \tag{4.17}$$

where $r_{ij}^2 = |\vec{r}_{ij}|^2$ and $\vec{r}_{ij} = \vec{r}_i - \vec{r}_j$ is the relative coordinate between anyons i and j.

The vector (gauge) potential associated with the i-th anyon is given by [8, 2, 9]

$$A_i(\vec{r}_i) = \alpha \sum_{i \neq j} \frac{\hat{z} \times \vec{r}_{ij}}{r_{ij}^2}, \tag{4.18}$$

where $\hat{z}$ is the direction perpendicular to the 2-dimensional space where the anyon quasiparticles reside. Here, α serves as the coupling constant, which

dictates the strength of the interaction between anyons in our system. This will allow us to consolidate the interactions between the anyons into the Hamiltonian.

As an aside, for fermions, such as electrons, $\alpha = 1$ corresponds to the strongest form of coupling in the way described above. On the other hand for bosons ($\alpha = 0$), we have no coupling between particles, which is reflected in Eqn. 4.18.

For the i-th anyon, the contribution to the Hamiltonian can be written as

$$\mathcal{H}_i = \frac{1}{2m}(p_i - A_i(\vec{r}_i))^2 + \frac{m\omega^2}{2}\vec{r}_i^{\,2}, \tag{4.19}$$

where the $p_i - A_i(\vec{r}_i)$ term represents the canonical momentum of the system. This is a required modification since we must account for the motion of the anyons in the presence of the gauge potential in addition to their mechanical momentum.

Then, with only essential coupling (minimal prescription) between the anyons by means of the gauge potential, the Hamiltonian for the N-anyon system in a harmonic potential is given by

$$\mathcal{H} = \frac{1}{2m}\sum_{i=1}^{N}(p_i - A_i(\vec{r}_i))^2 + \frac{m\omega^2}{2}\sum_{i=1}^{N}\vec{r}_i^{\,2}. \tag{4.20}$$

Substituting Eqn. 4.18 into Eqn. 4.20, this gives rise to

$$\mathcal{H} = \frac{1}{2m}\sum_{i=1}^{N}\vec{p}_i^{\,2} + \frac{m\omega^2}{2}\sum_{i=1}^{N}\vec{r}_i^{\,2} - \frac{\alpha}{2m}\sum_{i\neq j}^{N}\frac{\ell_{ij}}{r_{ij}^2} + \frac{\alpha^2}{2m}\sum_{i\neq j,k}^{N}\frac{\vec{r}_{ij}\cdot\vec{r}_{ik}}{r_{ij}^2 r_{ik}^2}, \tag{4.21}$$

where $\ell_{ij} = (\vec{r}_i - \vec{r}_j) \times (\vec{p}_i - \vec{p}_j)$ is the relative angular momentum of anyon i and j.

Chapter 5

To-Do List

- Finish/modify irreducible rep. example in Chapter 1.
- Lorentz group example?
- Probably should redo the Chapter 1 with nicer notation and stray away from Tung's notation when possible.

- Show $\psi_n(\sigma_i)$ invertible? Yes, eventually
- derive $\psi_n^{\mathbf{r}}(\sigma_i)$ matrices or state?
- Show $\psi_n^{\mathbf{r}}(\sigma_i)$ invertible? Yes, eventually
- Explicitly show why Burau isn't able to be made unitary?
- unitary matrices from B_n acting on $|\Psi\rangle$ (rotation of Hilbert space) example

---

- Go through vector stuff as in paper to connect the cross product stuff to the dot product stuff.
- Show the additional cross terms from $N = 2$ to $N = 3$ and beyond.
- Add paragraph on gauge theory/motivation.
- Anyons: fusion rules

- Anyons: τ anyon/Fibonacci anyon example. Relate to singlet/triplet states in spin-1/2 system.
- Anyons: 2 non-interacting anyons example
- Anyons: 2 non-interacting anyons in oscillator potential example
- Anyons: resolve 2- vs 3-anyon system Hamiltonian ("non-trivial braiding effects!")

References

[1] E. Artin. Theory of braids. *The Annals of Mathematics*, 48(1):101, January 1947.

[2] G. Date, M. V. N. Murthy, and Radhika Vathsan. Classical and quantum mechanics of anyons, 2003.

[3] Colleen Delaney, Eric C. Rowell, and Zhenghan Wang. Local unitary representations of the braid group and their applications to quantum computing, 2016.

[4] Avinash Deshmukh. An introduction to anyons.

[5] W. Fulton. *Algebraic Topology: A First Course*. Graduate Texts in Mathematics. Springer New York, 1997.

[6] Juan Gonzalez-Meneses. Basic results on braid groups, 2010.

[7] Christian Kassel and Vladimir Turaev. *Homological Representations of the Braid Groups*, page 93–150. Springer New York, 2008.

[8] Avinash Khare. *Fractional Statistics and Quantum Theory*. WORLD SCIENTIFIC, February 2005.

[9] K Moriyasu. *An Elementary Primer for Gauge Theory*. WORLD SCIENTIFIC, October 1983.

[10] Dale Rolfsen. Tutorial on the braid groups, 2010.

[11] Craig C. Squier. The burau representation is unitary. *Proceedings of the American Mathematical Society*, 90(2):199–202, 1984.

[12] Jean-Luc Thiffeault. The burau representation of the braid group and its application to dynamics. Presentation given at Topological Methods in Mathematical Physics 2022, Seminar GEOTOP-A, September 2022.

[13] Wu-Ki Tung. *Group theory in physics: An introduction to symmetry principles, group representations, and special functions in classical and quantum physics*. World Scientific Publishing, Singapore, Singapore, January 1985.